1 Numerical Discretization and Structure Preservation

In this work, we consider the scaled Korteweg–de Vries (KdV) equation. A **solitary wave** is a localized wave of translation that arises from a perfect balance between nonlinear steepening effects (convection) and linear spreading effects (dispersion). It travels at a constant velocity and retains its shape indefinitely in the absence of external perturbations or boundaries. The governing equation is:

$$u_t + (u^2)_x + 6u_{xxx} = 0,$$

which can be written as an infinite-dimensional Hamiltonian system

$$u_t = J\frac{\delta H}{\delta u},$$

where

$$J = -\partial_x$$

is a skew-adjoint differential operator, and the Hamiltonian functional is given by

$$H[u] = \int \left(\frac{u^3}{3} - 3u_x^2\right) dx.$$

For this Hamiltonian, the variational derivative is

$$\frac{\delta H}{\delta u} = u^2 + 6u_{xx},$$

and therefore

$$u_t = -\partial_x \left(u^2 + 6u_{xx}\right) = -(u^2)_x - 6u_{xxx},$$

which is exactly the equation under consideration.

This equation is a rescaled form of the standard KdV equation and is adopted here because it is directly consistent with the Hamiltonian functional and the numerical implementation used in this work.

For reliable long-time computations, naive discretizations are often insufficient, since they may introduce artificial numerical dissipation or dispersion and gradually destroy qualitative wave features such as shape preservation and phase shifts during collisions. Therefore, the numerical scheme should preserve the underlying geometric structure as much as possible, in particular the skew-symmetry of the operator J and the Hamiltonian structure of the semi-discrete system.

We achieve this by first transforming the continuous Hamiltonian PDE into a discrete Hamiltonian system of ordinary differential equations (ODEs) through a structure-preserving spatial discretization, and then applying suitable geometric time integrators for the temporal evolution.

1.1 Case 1: Periodic Boundary Conditions

We first consider the equation on a bounded spatial domain $x \in [-L/2, L/2]$ with periodic boundary conditions.

1.1.1 Spatial Discretization

We introduce a uniform grid with N points and step size $h = L/N$. The continuous function $u(x,t)$ is approximated by the discrete vector

$$U(t) = [u_1(t), u_2(t), \ldots, u_N(t)]^T.$$

The continuous skew-adjoint operator $J = -\partial_x$ is approximated by the discrete operator

$$J_h = -D_1,$$

where D_1 is the central finite difference matrix with periodic boundary conditions:

$$D_1 = \frac{1}{2h}\begin{pmatrix} 0 & 1 & 0 & \ldots & -1 \\ -1 & 0 & 1 & \ldots & 0 \\ \vdots & \ddots & \ddots & \ddots & \vdots \\ 0 & \ldots & -1 & 0 & 1 \\ 1 & \ldots & 0 & -1 & 0 \end{pmatrix}.$$

A crucial property of D_1 is that it is skew-symmetric, that is,

$$D_1^T = -D_1.$$

Hence,

$$J_h^T = -J_h,$$

so the discrete operator preserves the geometric structure of the continuous one.

The discrete Hamiltonian is defined by replacing the integral with a Riemann sum and the spatial derivative with the finite difference operator:

$$H_h(U) = h \sum_{i=1}^{N} \left(\frac{U_i^3}{3} - 3(D_1 U)_i^2 \right).$$

The resulting semi-discrete system is a finite-dimensional Hamiltonian ODE of the form

$$\dot{U} = J_h \nabla H_h(U).$$

In the implementation, the discrete gradient is evaluated consistently with the continuous variational derivative as

$$\nabla H_h(U) \approx (U_1^2, \ldots, U_N^2)^T + 6 D_2 U,$$

where D_2 denotes the second-order difference operator.

1.1.2 Temporal Discretization: The Implicit Midpoint Rule

To integrate the Hamiltonian ODE system in time, we use the Implicit Midpoint Rule. For a time step Δt, the method is given by

$$\frac{U^{n+1} - U^n}{\Delta t} = J_h \nabla H_h \left(\frac{U^{n+1} + U^n}{2} \right).$$

The Implicit Midpoint Rule is a symplectic integrator. For Hamiltonian systems, it is well known for its excellent long-time stability properties, keeping the discrete energy error bounded without secular drift.

Because the method is implicit and the gradient ∇H_h contains nonlinear terms, evaluating U^{n+1} requires solving a nonlinear algebraic system at each time step. We define the residual function:

$$F(U^{n+1}) = U^{n+1} - U^n - \Delta t J_h \nabla H_h \left(\frac{U^{n+1} + U^n}{2} \right) = 0.$$

To find the root of this system, we employ the Newton–Raphson iteration method. Let $U^{(k)}$ be the k-th iterative approximation of U^{n+1}. The update step is given by solving the linear system:

$$\mathcal{J}_F(U^{(k)}) \delta U = -F(U^{(k)})$$

$$U^{(k+1)} = U^{(k)} + \delta U$$

where the Jacobian matrix $\mathcal{J}_F$ is defined as:

$$\mathcal{J}_F(U) = I - \frac{\Delta t}{2} J_h \nabla^2 H_h \left(\frac{U + U^n}{2} \right).$$

Here, $\nabla^2 H_h$ represents the Hessian matrix of the discrete Hamiltonian, evaluated at the midpoint. The iteration proceeds until the L_2 norm of the residual $F(U^{(k)})$ falls below a strict tolerance threshold, ensuring the symplectic structure is preserved at each step.

1.2 Case 2: Reflective Boundary Conditions

We next consider a finite domain with natural or reflective boundary conditions. In this setting, the periodic central difference matrix cannot be directly used at the boundary without affecting the skew-symmetric structure.

To address this difficulty, we employ a Strang operator splitting method. The equation

$$u_t + (u^2)_x + 6 u_{xxx} = 0$$

is decomposed into two sub-problems: a nonlinear convection part and a linear dispersion part.

1. **Nonlinear convection:**

$$u_t + (u^2)_x = 0.$$

   This part is solved over a half-time step $\Delta t/2$ using the Implicit Midpoint Rule.

2. **Linear dispersion:**

$$u_t + 6u_{xxx} = 0.$$

A skew-symmetric discrete operator L_{mat} is constructed for the dispersive term, and the resulting linear system is advanced over a full time step Δt using the Crank–Nicolson method. Because L_{mat} is skew-symmetric, the Crank–Nicolson step preserves the discrete L^2 norm of the linear subproblem.

3. **Nonlinear convection:** A final half-time step $\Delta t/2$ is applied to complete the Strang splitting cycle.

This splitting strategy allows us to handle reflective boundary effects in a stable way while preserving the geometric structure of the subproblems as much as possible.

2 Numerical Experiments and Visualization

To verify the structure-preserving properties of the proposed discretizations, we perform numerical experiments for both cases.

2.1 Single Soliton Propagation and Error Analysis

Using the implicit midpoint method under periodic boundary conditions, we simulate the propagation of a single solitary wave. The initial waveform is depicted in Figure 1.

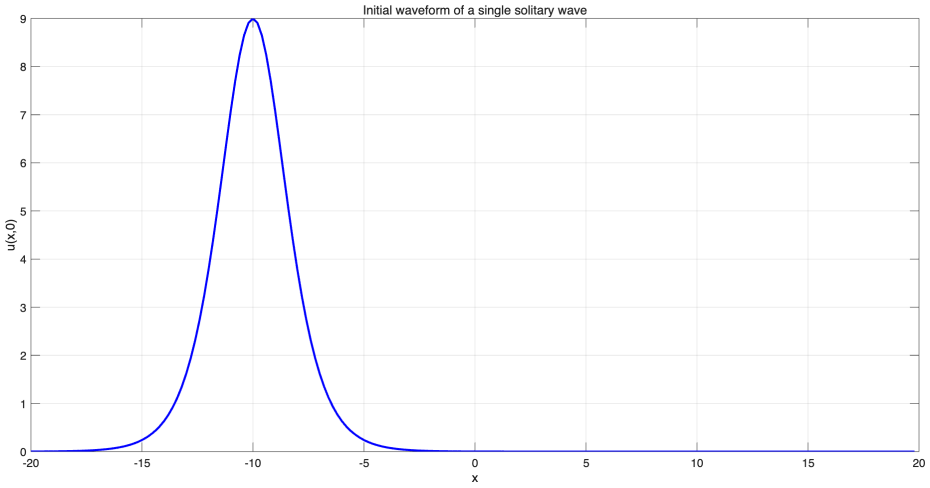

Figure 1: Initial waveform of a single solitary wave at $t = 0$.

We then observe the time evolution of the wave and monitor the Hamiltonian error. As shown in Figure 2, the numerical energy error remains bounded and exhibits non-dissipative behavior over time, indicating that the structure of the solution is well preserved throughout the simulation.

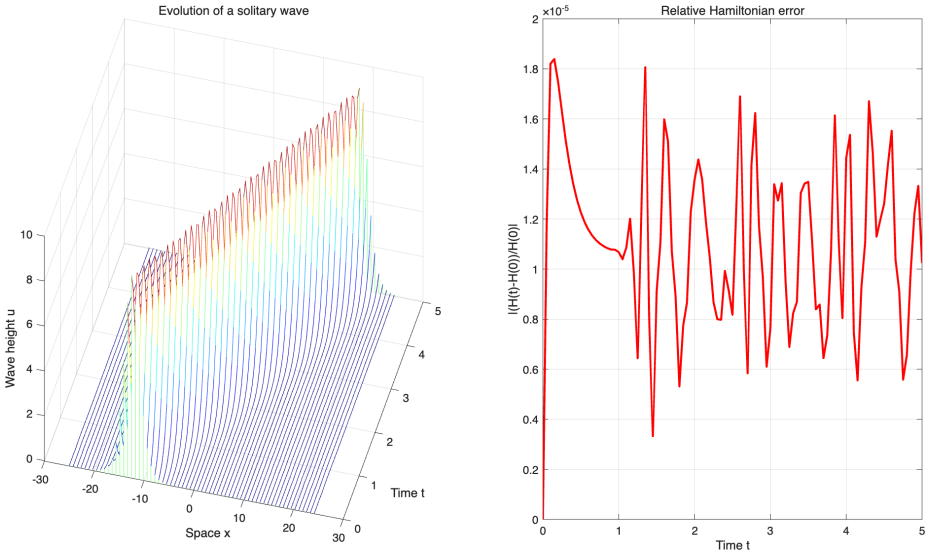

Figure 2: Left: Spatiotemporal evolution of the solitary wave. Right: Relative error of the Hamiltonian over time, showing bounded fluctuations without secular drift.

To further assess the accuracy and stability of the temporal discretization, we carry out a convergence study using different time step sizes Δt.

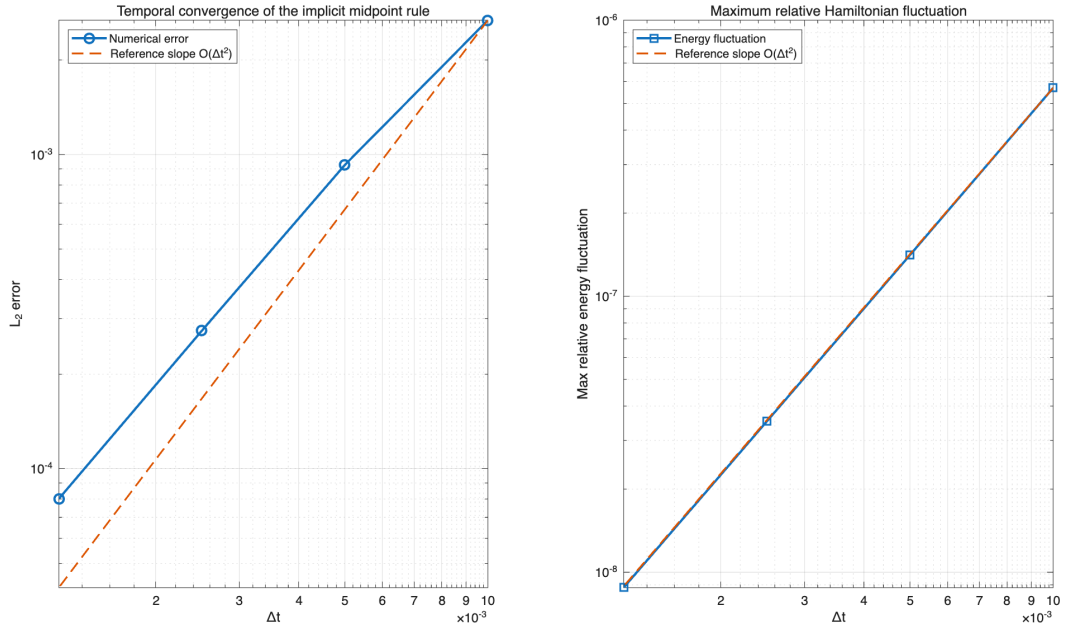

Figure 3: Convergence of the L_2 error (left) and relative Hamiltonian error (right) for the Implicit Midpoint Rule. The left panel confirms the expected second-order convergence of the solution error, while the right panel shows that the Hamiltonian fluctuation decreases consistently as Δt is refined.

2.2 Two-Soliton Elastic Collision

A characteristic feature of KdV equations is the nearly elastic interaction of multiple solitary waves. Because the propagation speed of a KdV solitary wave is strictly proportional to its amplitude, a taller wave will always travel faster than a shorter one. To study this phenomenon, we initialize the domain with a faster and taller wave trailing a slower and shorter one.

During the interaction, the larger wave overtakes the smaller one. They do not permanently unite; rather, they temporarily merge into a composite waveform during the collision before separating again. After the interaction, both waves re-emerge, completely recovering their original shapes, amplitudes, and velocities. The only lasting footprint of this collision is a phase shift: the faster wave is shifted forward, and the slower wave is shifted backward relative to the trajectories they would have taken had no interaction occurred.

To visualize this interaction, we present both a space-time contour plot and a sequence of solution snapshots.

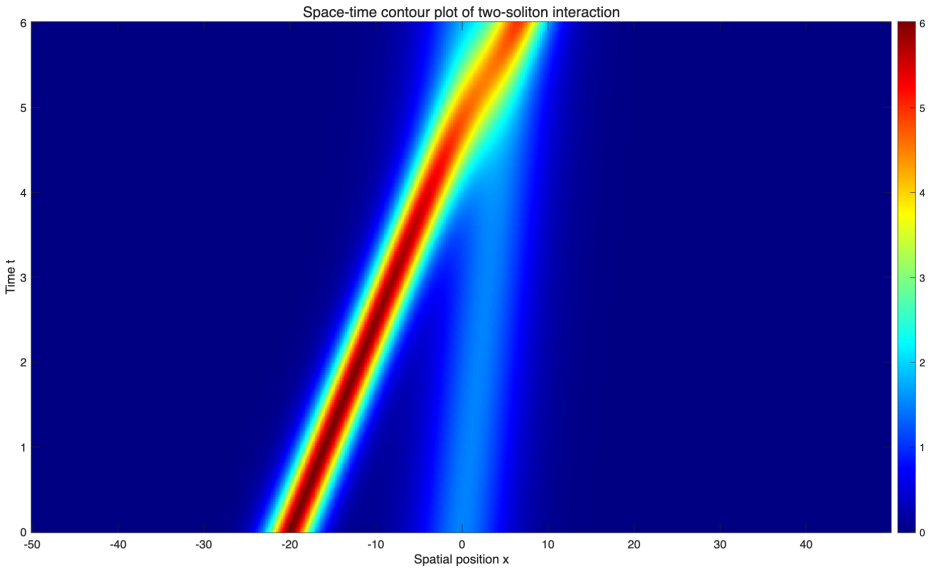

Figure 4: Space-time contour plot of the two-soliton interaction. The slopes of the high-intensity trajectories reflect the propagation speeds of the two waves. A visible phase shift appears near the interaction region, illustrating the nonlinear wave dynamics.

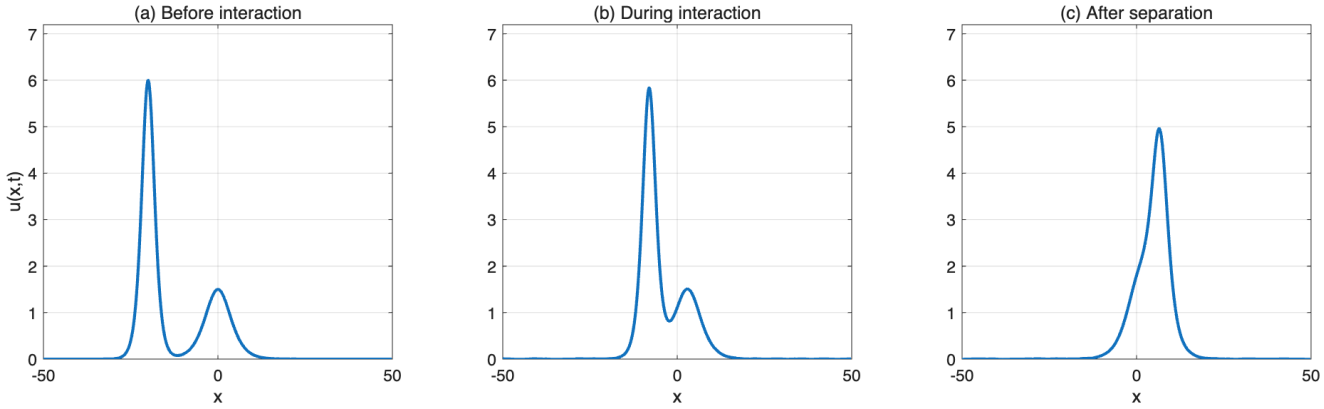

Figure 5: Chronological snapshots of the interaction process: (a) before collision, (b) during collision, and (c) after separation. The waves recover their main shapes and amplitudes after interaction, indicating the structure-preserving quality of the numerical scheme.

2.3 Boundary Reflection Dynamics

To test the splitting method in a non-periodic setting, we initialize a solitary wave near a reflective boundary.

When a solitary wave interacts with a reflective boundary, it cannot pass through. Unlike periodic boundaries where the wave simply wraps around the domain, the reflective boundary forces the wave energy to propagate backward. However, because a true solitary wave requires a strictly forward-moving balance of nonlinearity and dispersion in the KdV equation, the reflected wave loses its pure solitary nature. The interaction with the wall effectively breaks the wave down, causing it to reflect as a train of high-frequency dispersive ripples moving in the opposite direction.

This complex reflection dynamic introduces specific numerical challenges. To maintain stability and accurately resolve the high-frequency dispersive waves generated at the boundary, the time step Δt generally needs to be decreased. While the Crank–Nicolson scheme used for the linear dispersion part is unconditionally stable in the L_2 norm, taking too large a time step leads to severe dispersion errors (numerical ringing). Therefore, a smaller Δt is required to suppress artificial oscillations and capture the physical reflection dynamics accurately.

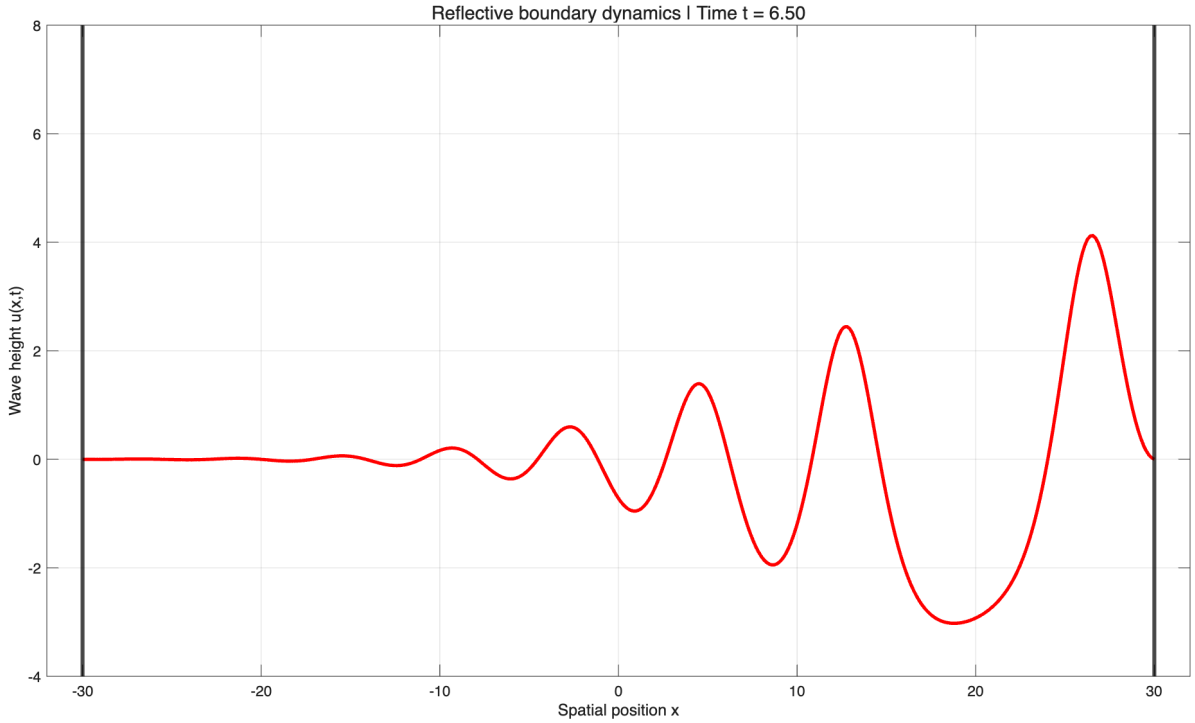

Figure 6: Boundary-induced wave behavior near a natural boundary. The operator splitting method captures stable reflection-like dynamics while maintaining numerical stability.